Digital Object Identifier: 10.1109/ULTSYM.2008.0253

The Physical Acoustics of Energy Harvesting

Stewart Sherrit
Jet Propulsion Laboratory, California Institute of Technology
4800 Oak Grove, Pasadena, CA, 91109

Abstract – **Energy harvesting systems based on the transformation of acoustic vibrations into electrical energy are increasingly being used for niche applications due to the reduction in power consumption of modern day electronic systems. Typically these applications involve extracting energy at remote or isolated locations where local long term power is unavailable or inside sealed or rotating systems where cabling and electrical commutation are problematic. The available acoustic power spectra can be in the form of longitudinal, transverse, bending, hydrostatic or shear waves of frequencies ranging from less than a Hz to 10's of kHz. The input stress/vibration power can be generated by machines, humans or nature. We will present a variety of acoustic energy harvesting modes/devices and look at the commonalities of these devices. The common elements of these systems are: an input mechanical power spectrum, an effective acoustic impedance matching, a conversion of the input mechanical energy into electrical energy using piezoelectric or biased electrostrictive transducers and a matched electrical load. This paper will focus of the physical acoustics of these energy harvesting systems and identify the elements of these devices and look at the current limits of the harvested electrical power from these devices. Recent results on an acoustic electric feed-through device demonstrated acoustic power conversions of the order of 70 W/cm^2 and 25 W/cm^3 using a pre-stressed stacked PZT ceramics operating at 16 kHz with an efficiency of 84%. These results suggest the piezoelectric is not the limiting element of these devices and we will show that the main impediment to increased power is the vibration source amplitude, frequency, inertia and the size limitations of the energy harvesting systems or in the case of human powered systems the requirement that the device remains unobtrusive. Although the power densities of these devices may be limited there are plenty of applications that are feasible within the available power densities due to the wonders of CMOS.**

Keywords: Piezoelectric Transduction, Energy Harvesting, Energy Scavenging, Active Damping, Autonomous sensing

1. INTRODUCTION

A variety of applications exist where power developed using piezoelectric energy harvesting transducers offer a potential advantage over other power generating technologies[1,2,3,4,5]. These systems convert various forms of mechanical vibrations into AC electrical signals which can be conditioned[5,6,7,8] to supply DC power to a load or device. The major competing technology for energy harvesting using the piezoelectric effect is the solar cell. These systems can generate a few mW/cm^2 on average[9] and up to 100 mW/cm^2 in bright sunlight[2] and are continually improving in both efficiency and cost per Watt[10]. In order for piezoelectric generators to compete they must have: 1) A large acoustic power density in the structure such that the generated power density exceeds photovoltaics, 2) Require operation in enclosed regions (ex. buildings, tunnels, automobiles), 3) Moving structures (ex. Rotating systems). It also may be that the system requires constant power generation not effected by the seasonal, nocturnal or local weather variations. Another advantage of these generators that may have applications to large space structures is that when combined with wireless technology such as RFID they can reduce the need for cabling or commutation in rotating structures. These devices have been proposed for a variety of niche applications from powering tire pressure sensors[4], Mobile electronic devices[2], medical implants[1,11], Shoe power[3], Powering RFID sensor nodes[12]. In addition a variety of energy harvesting systems have been develop using a wide range of transducer types and piezoelectric or electrostrictive materials. Many vibration modes can be used to generate the electrical power. Figure 1 shows examples of common isolated modes of excitation of piezoelectric transducers that can be mounted on or to a structure. These include extensional, transverse, shear and hydrostatic excitation. Each mode is shown with a reaction mass however it could be clamped to a structure increasing the elastic energy density over the kinetic. In order to investigate the physical acoustics of these structures we will initially confine our analysis to the thickness mode transducer and look at how modifications to this structure can be applied to other transducer configurations.

In order to proceed in investigating these mechanisms we make some simplifying assumptions about the vibrating structures we are scavenging or harvesting energy from. We do this by assuming that at the interface, the vibrations are either force or displacement limited. The true boundary conditions will depend on the relative mass and stiffness of the structure and harvester. In a real world application this is likely the difficult information to assess without measuring. For simple structures the power density in the structure could be approximated by using an acoustic element. For a stiff large mass structure with vibration amplitude δ_o, the total power defined as the time rate of change of the kinetic energy in the structure is found to be $P = \delta_o^2 m\omega^3$. That is, for a given vibration amplitude the power increases with a cube of the frequency. Alternatively if the structure is driven by a force F_o and is force limited then the

total power amplitude $P = F_o^2/(m\omega)$ decreases as the frequency and mass increases since the peak force is $F_o = m\delta_o\omega^2$ (δ_o decreases as the inverse of the square of the frequency). In the case of a harvester that is clamped with respect to some structure the power is $P=F_o^2\omega t/YA$ for a fixed force F_o and $P= YA\delta_o^2\omega/t$ for the case where δ_o is fixed. Y is Young's Modulus of the structure. In general the peak power density has both elastic and kinetic components and is not single frequency and may be represented by a frequency spectrum.

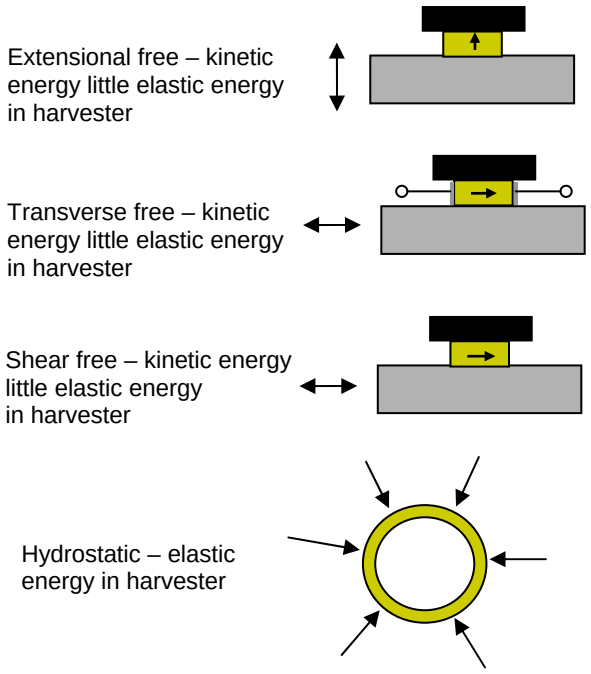

Figure 1. Basic piezoelectric energy harvesting modes of excitation. The mass element could be replaced by a clamping structure which would increase the elastic energy density.

Schematics diagrams of two of the simplest conceivable configurations of these piezoelectric harvesters are shown in Figure 2. The top figure show a piezoelectric plate (poled in the thickness direction) clamped between two elements with a force in the thickness direction F(ω). This configuration is embedded between two structures and since the opposite surface is clamped the voltage generated in the open circuit case is found to be

$$V(\omega) = \frac{e_{33}F(\omega)\omega\mathbf{Z}}{c_{33}^D} \quad (1)$$

Where e_{33} is the piezoelectric charge constant, $\boldsymbol{Z}$ is the parallel combination of the clamped capacitance and load resistance R_L and c_{33}^D is the open circuit elastic stiffness. The open circuit voltage in the reaction mass configuration in low frequency range is

$$V(\omega) = \frac{e_{33}\delta_o\omega^2 m\omega\mathbf{Z}}{c_{33}^D} \quad (2)$$

Where δ_o is the surface displacement and m is the sum of half the piezoelectric mass and reaction mass. In the open circuit limit ($R_L=\infty$) the clamped case a) is essentially a harmonic force sensor while the reaction mass configuration b) is similar in configuration to a piezoelectric accelerometer. In the short circuit limit one should replace c_{33}^D with c_{33}^E. The short and open circuit elastic constants are bounding conditions and the actual elastic constant with a load resistance R_L is between these two values. Other transducers which have similarities in the physical acoustics include active damping transducers [13,14], piezoelectric transformers and acoustic electric feed-throughs [15,16,17,18]. Medical ultrasound although generally at much higher frequencies also has many of the same issues with regards to transducer optimization. The fact that the structure in 1a) is bonded between two structural elements requires that harvesters of this type be designed into the structure or the structure can be retrofitted to accommodate this type of harvester (example piezoelectric washer). An alternate harvester configuration that can be clamped, bolted or bonded to a free surface of a vibrating structure is shown in the Figure 2 b). This structure has a reaction mass to increase the load experienced by the piezoelectric.

2. THEORY

a) Standard Models

In order investigate the performance of energy harvesters based on acoustic vibrations we use the simple concepts shown in Figure 2 and apply Mason's equivalent network[19] with complex coefficients[20]. A schematic of the circuit for this model is shown in Figure 3. The variables are voltage and current on the electrical side of the transformer and force and velocity on the mechanical side of the transformer. A stress free surface is represented as a short on the acoustic port while a clamped surface is represented as an open circuit. In order to model layers one uses the transmission line element of an acoustic layer as shown in Figure 4 and described by Redwood[21] and McSkimmin[22].

The parameters of Mason's equivalent circuit are shown in Table 1. We have chosen the material constants of CTS 3203HD (formerly Motorola 3203HD) for the modeling because it is well characterized [23,24]. The constants for the thickness mode and the transducer geometry for the models are shown in Table 2. We report peak power densities across a real load which is equal to twice the average power.

The impedance of the acoustic layer shown in Figure 4 when the right mechanical port is stress free (short the terminals) reduces to

$$Z_A(\omega) = i\rho Av\tan\left(\frac{\omega L}{v}\right) \quad (3)$$

In addition in the low frequency limit the impedance shown in equation 3 reduces to $Z(\omega) = i\rho AL\omega = im\omega$. Also in the Limit $L\rightarrow\infty$ the acoustic impedance $Z(\omega)\rightarrow \rho Av$, the radiation impedance. The velocity as seen from the input port (left

side) in figure 4 is plotted in Figure 5 for the case where the output port is stress free (shorted) or clamped (open).

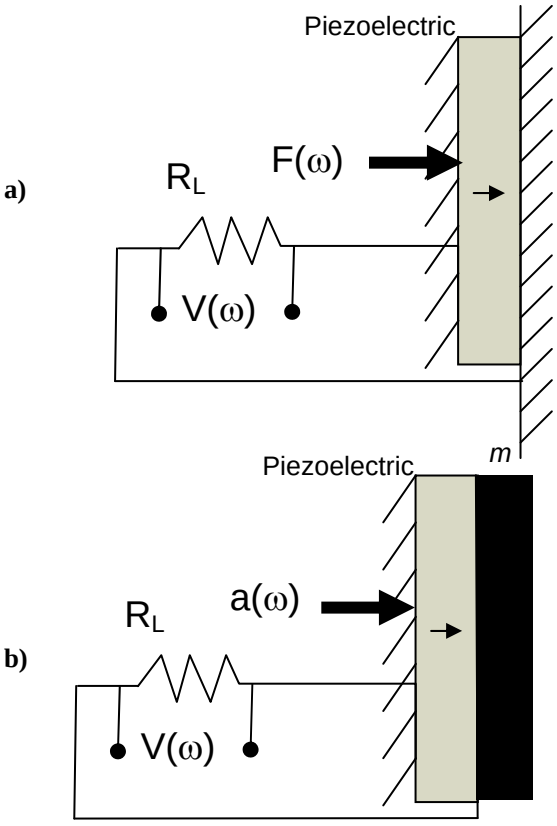

Figure 2. Basic piezoelectric energy harvesting systems. a) A structure applies a harmonic Force F(ω) to the surface of a piezoelectric material which is clamped on the opposite side. b) A structure applies a harmonic acceleration a(ω) to the surface of a piezoelectric material which has a reaction mass *m* on opposite surface. A harmonic voltage is generated across the piezoelectric and load resistance R_L.

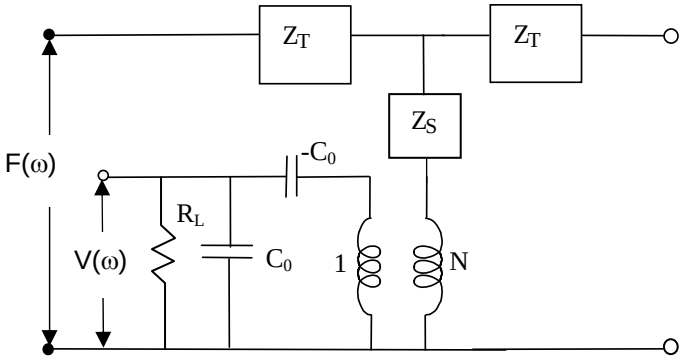

Figure 3. Circuit model of a basic piezoelectric energy harvesting systems. a) A structure applies a harmonic Force F(ω) to the surface of a piezoelectric material which is clamped on the opposite side.

In the figures we see that in the stress free case the layer initially (low frequency) acts as an inductor with the inductance proportional to the mass. In the clamped case the impedance initially (low frequency) is capacitive with the capacitance proportional to the stiffness and the product of the Area to thickness ratio. At higher frequencies the impedance in both the clamped and free case goes through their respective resonance.

In Figure 6 we show the electromechanical model for the case of a piezoelectric and reaction mass mounted on a structure where the structure surface harmonic velocity is $v(\omega)=a(\omega)/\omega$.

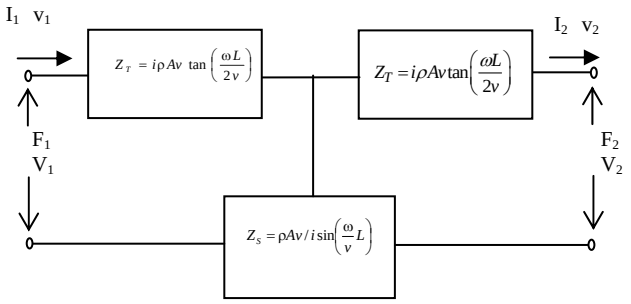

Figure 4. Equivalent circuit for a layer attached to the transducer. ρ, *A*, *L*, and *v* are the density, area, thickness, and acoustic velocity of the layer. *v* can be complex to account for attenuation.

The acoustic impedance Z_A is defined using equation 3 and the properties of the reaction mass. In order to compare the clamped and free models in off resonance excitation we evaluate the two models at 1 kHz for force of 50 N and a velocity of 1.0 m/s. In the free model we have a choice for the length and material of the reaction mass if we fix the area to that of the piezoelectric. This model assumes that the harvester structure does not stiffen the vibrating structure and is lightweight in comparison to the structure. If we were to make $v(\omega)$=constant this means that the acceleration $a(\omega)$ increases with frequency.

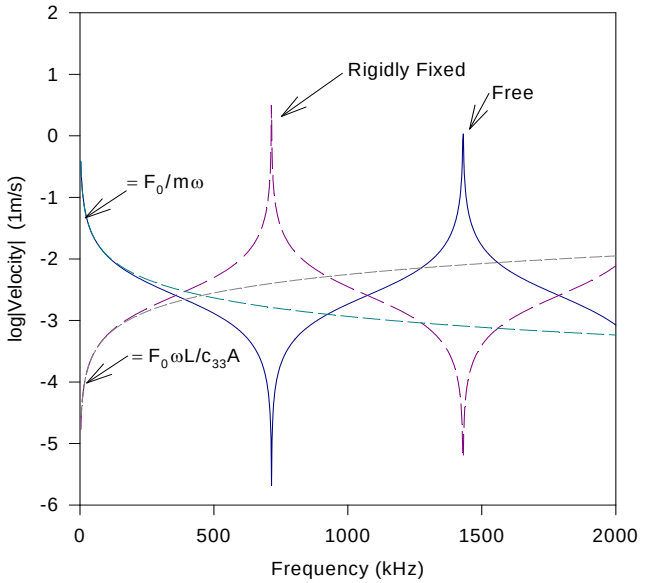

Figure 5. The amplitude of the input velocity for a harmonic force with amplitude F_o for the acoustic layer shown in figure 4 in the stress free and clamped condition.

In Figure 7 we plot the peak power density obtainable as a function of the load resistance in the clamped case for a 50 N harmonic force. The maximum peak energy

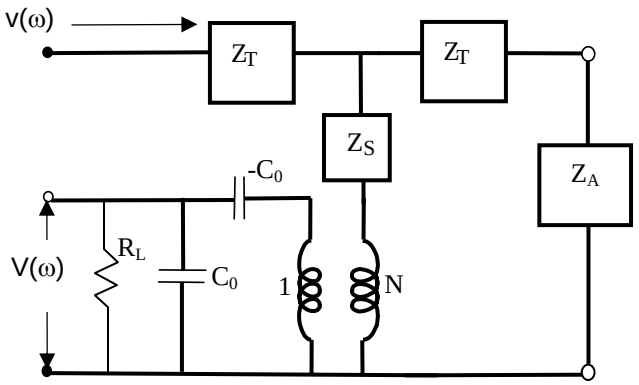

Figure 6. Circuit model of a piezoelectric energy harvesting system. A structure applies a harmonic velocity v(ω) to the surface of a piezoelectric material which has a reaction mass *m* on opposite surface.

density is 321 μW/cm^2 at a load resistance of 225 kΩ. At low resistance R_L the power determined from Mason's model is controlled by the short circuit elastic constant (Power determined from equation 1 with c_{33}^E) while at impedances larger that the peak power impedance the curve follows the open circuit equation (Power determined from equation 1 with c_{33}^D). The max power is bounded by the open and short circuit equations. The total power delivered to the device with a force amplitude of 50 N at 1 kHz is 2.16 mW while the total dissipated power is 361 μW giving a power conversion efficiencies of 89% or 14.9% depending on whether you define the efficiency in terms of the dissipated or total power.

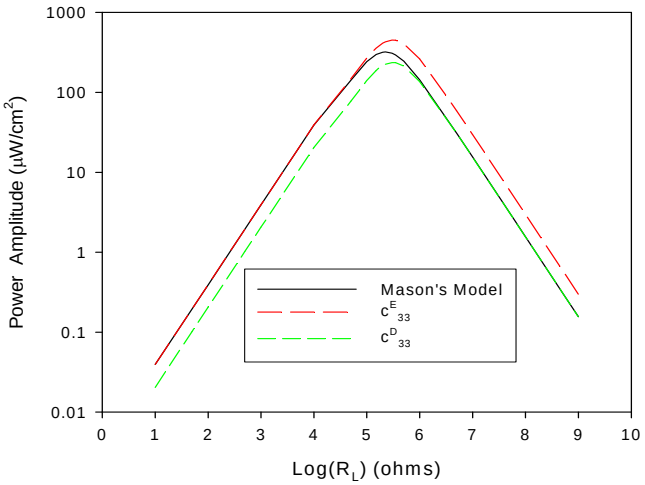

Figure 7. The log of power amplitude as a function of the log of the load resistance R_L for the clamped piezoelectric with material properties and geometry shown in Table 2. The force was 50 N and the frequency 1 kHz.

The load for maximum power scales inversely with frequency so at 4 kHz the load for maximum power is 56.3 kΩ. The stress on the piezoelectric is 0.5 MPa which is a factor of about 40 below the normal pre-stress that one applies to high power actuators. This means that in theory for a structure with a large surface area exerting 0.5 MPa/cm^2 one could funnel the stress to a contact area 40 times smaller to increase the stress in the piezoelectric to its pre-stress values. This could produce at 1 kHz power densities of the order of 0.5 W/cm^2 at similar efficiencies.

In Figure 8 we show the same curve for the case of a bare free harvester and harvesters driven at 1 m/s and 1 kHz with reaction masses using Titanium, Stainless Steel and Tungsten. The lengths are adjusted to give the same power–load resistance curves found in Figure 7 for the clamped harvester. The material properties and lengths are shown in Table 3. We have assumed a Q of 1000 for each of these materials. Since the Q of the piezoelectric is lower by a factor of 10 and most of the energy is kinetic this suggests that both the max power density and power efficiency should not be affected significantly by this assumption.

In the case of the bare free resonator we see that there is a reduction in the power density as expected since the only forces being exerted on the piezoelectric are due to the reaction of half the piezoelectric mass. That is the acoustic impedance of the piezoelectric can be modeled with an imω with m being the sum of half the piezoelectric mass and the reaction mass (ie, the density time length in Table 3 is a constant).

Table 1. Complex parameters of Mason's equivalent circuit

Mason's Model

$$\mathbf{C}_0 = \frac{\boldsymbol{\varepsilon}_{33}^S A}{t} \qquad \mathbf{N} = \mathbf{C}_0 \boldsymbol{h}_{33}$$

$$\boldsymbol{Z}_0 = \rho A \mathbf{v}^D = A\sqrt{\rho\, \mathbf{c}_{33}^D} \qquad \boldsymbol{\Gamma} = \frac{\omega}{\mathbf{v}^D} = \omega\sqrt{\frac{\rho}{\boldsymbol{c}_{33}^D}}$$

$$Z_T = i\mathbf{Z}_0 \tan(\boldsymbol{\Gamma} t/2) \qquad Z_S = -i\mathbf{Z}_0 \csc(\boldsymbol{\Gamma} t)$$

Table 2. Complex material constants determined from a average of 5 samples for Motorola 3203HD material[25,26].

Material Constants and Geometry of Piezoelectric Material (Motorola 3203HD)
ρ = 7700 kg/m^3 t = 0.002 m Diameter = 0.01128 m
$\mathbf{c}_{33}^D$ (x 10^{11} N/m^2) = 1.74(1 + 0.01i)
$\boldsymbol{\varepsilon}_{33}^S$ (x 10^{-8} F/m) = 1.02 (1 - 0.065i)
$\boldsymbol{h}_{33}$ (x 10^9 V/m) = 2.17 (1 + 0.067i)
$\boldsymbol{k}_t$ = 0.526 (1 + 0.0296i)

The power conversion efficiencies for the mass loaded harvester are similar for the ratio of converted power to dissipated power and are about 87% -88%. However in these harvesters the reactive part of the complex power is large and of the order of 50 W peak due to the cycling of the kinetic energy of the reaction mass. In both the clamped and free

case the load impedance of maximum power transfer is found to be high (225 kΩ) for a 1 kHz excitation. In the low frequency range the peak power conversion efficiency is shown in Figure 9 for the various harvesters. We could reduce the thickness of the piezoelectric but this would also reduce the maximum peak power proportionally. Another approach is to use multi-layers.

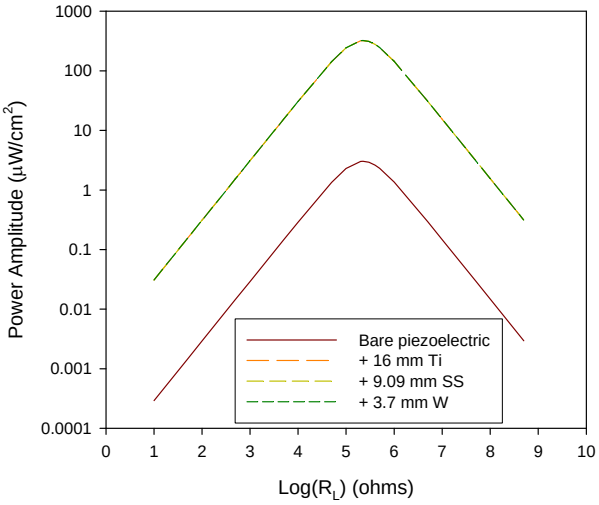

Figure 8. The power density as a function of the load resistance on the electrical port for a bare 2 mm piezoelectric and a piezoelectric with various materials of lengths as shown in Table 3.

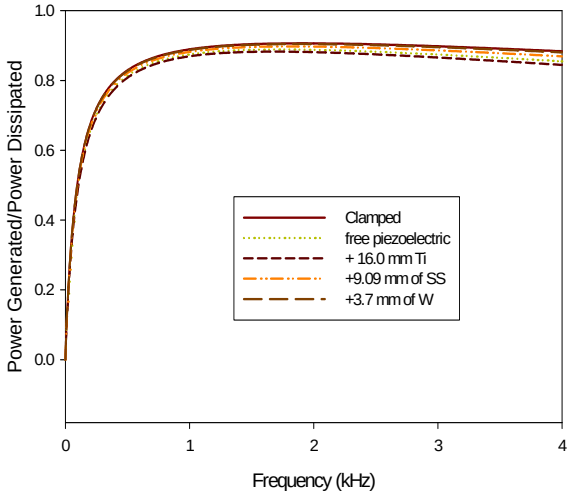

Figure 9. The power transfer efficiency calculated by maximizing the power at 1 kHz for various harvester configurations. The slight drop away from 1 kHz is due to the change in the source impedance with frequency. We have essentially tuned to match at 1 kHz.

Table 3. Material properties[27] and lengths of the reaction mass used to generate the peak power curves shown in Figure 8.

Material	V_L (m/s)	ρ (kg/m^3)	Length (mm)
Titanium	6100	4480	16.0
Steel	5800	7900	9.09
Tungsten	5200	19400	3.70

b) Multi-layers

In order to reduce the source impedance and maintain the power density level one could use multilayers. For one or two layers one can use the models in Figures 3 and 6. As n increases above 2 the acoustic wave travels more and more under short circuit conditions until about n=8 when the transition is complete[28,29,30]. Above n=8 the constants of the circuits shown in Figures 3 and 6 have to be modified. Mason's parameters for the multilayer are shown in Table 4 where n is the number of layer (n>8).

Table 4. Complex parameters of Mason's equivalent circuit for a thickness mode multilayer ($-C_0$ term is set to zero)

Mason's Model-Multilayer

$$\varepsilon_{33n}^S = n^2\varepsilon_{33}^S,\ h_{33n} = h_{33}/n,\ c_{33n}^D = c_{33}^D,\ c_{33n}^E = c_{33}^E$$

$$\mathbf{C}_0 = \frac{\boldsymbol{\varepsilon}_{33}^S A}{t} \qquad \mathbf{N} = \mathbf{C}_0 \boldsymbol{h}_{33}$$

$$\mathbf{Z}_0 = \rho\, A\mathbf{v}^E = A\sqrt{\rho\, \mathbf{c}_{33}^E} \qquad \boldsymbol{\Gamma} = \frac{\omega}{\mathbf{v}^E} = \omega\sqrt{\frac{\rho}{\mathbf{c}_{33}^E}}$$

$$Z_T = i\mathbf{Z}_0 \tan(\boldsymbol{\Gamma} t/2) \qquad Z_S = -i\mathbf{Z}_0 \csc(\boldsymbol{\Gamma} t)$$

If we use n=20 we find the peak power versus load resistance curves in Figure 10. The multilayer has the effect of reducing the load resistance for maximum peak power density by a factor of $\approx n^2$. In the clamped and free cases discussed previously the load resistance at maximum power was 225 kΩ compared to 562 Ω for the multilayer. The peak power density is found to be 320 μW/cm^2. The models we have used are also directly applicable to the length and thickness shear mode multilayers and the same factors would be found for k_{33} and k_{15}. Using a multilayer also increases the source capacitance to a level that at low frequencies may be tuned using an inductor of reasonable value to counteract the static capacitance and reduce the reactive power in the electrical port.

In the three cases of the free multilayer piezoelectric with reaction mass a series inductor of 124 mH and a load resistance of 223 Ω increases the peak power density across the load to 727 μW/cm^2. However the device is now tuned to the 1 kHz signal and both the total power density and power transfer efficiency decreases as the frequency is adjusted from the 1 kHz value. It should be emphasized that we have not tried to optimize the harvesters above. For example assuming the harvester was pre-stressed to the structure at a level of 30 MPa and we did not want to exceed this level the maximum power density at 1 kHz for the L tuned tungsten backed piezoelectric multilayer could be increased to 2 W/cm^2 if we increased the diameter of the tungsten diameter by a factor of two and increase the length of the tungsten reaction mass to 0.05 m (0.39 kg). For this larger mass even if we reduced the velocity to 0.1 m/s and removed the tuning we could generate a peak power of 11 mW/cm^2. It is interesting to note that for

these devices the material losses have small effect on the peak output power density for nominal PZT loss factors. In the lossless case the power density is 900 $\mu W/cm^2$ for the tuned multilayer A doubling of the dielectric loss and a factor of 10 decrease in the mechanical Q of the material constants shown in Table 2 reduces the generated power densities by about 18% percent.

c*) Resonance clamping*

In the free piezoelectric harvester we used a reaction mass to increase the force experienced by the piezoelectric as it is vibrated harmonically. The reaction mass is the low frequency limit of the full acoustic impedance shown in equation 3. At higher frequencies this impedance cycles between maximums and minimums as the argument of the tan function cycles through $n\pi/2$ and $n\pi$ where n is an integer. Rather than a mass load one could design a purely mechanical low frequency resonance structure (bender, mass-spring, flextensional spring, etc on the free face of the piezoelectric that has a maximum in the acoustic impedance at the frequency of interest which reacts against the piezoelectric at a specific frequency band.

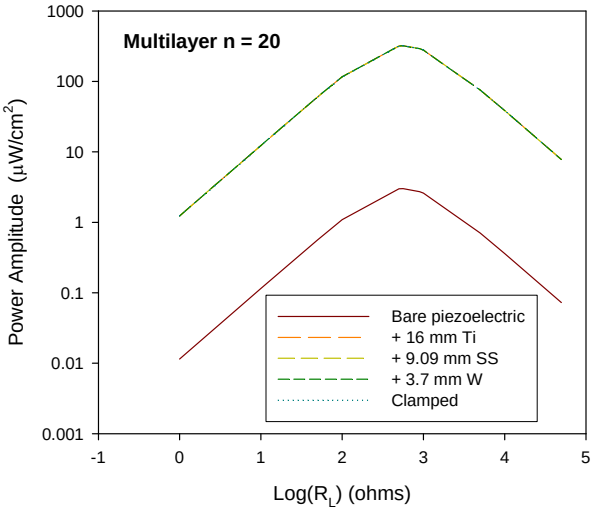

Figure 10. The power density as a function of the load resistance on the electrical port for a clamped multilayer piezoelectric and bare 2 mm multilayer piezoelectric and with reaction masses of various materials of lengths as shown in Table 3. All curves except the bare piezoelectric overlap.

Another approach that is commonly used to enhance the power density over a limited bandwidth is to design a low frequency piezoelectric transducer. Schematic diagrams of common resonators that can be designed in a compact form to resonate at lower frequencies are shown in Figure 11. These include series and parallel bimorphs[31,32,33] flextensional actuators[34], Cymbals[35], and monomorphs such as the Rainbows[36], Cerambows[37], and Thunder[38]. Similar analysis of these resonator types can be performed with electromechanical models[39,40,41] of these resonators. In these devices the stress levels increase as the Q of the resonator increases.

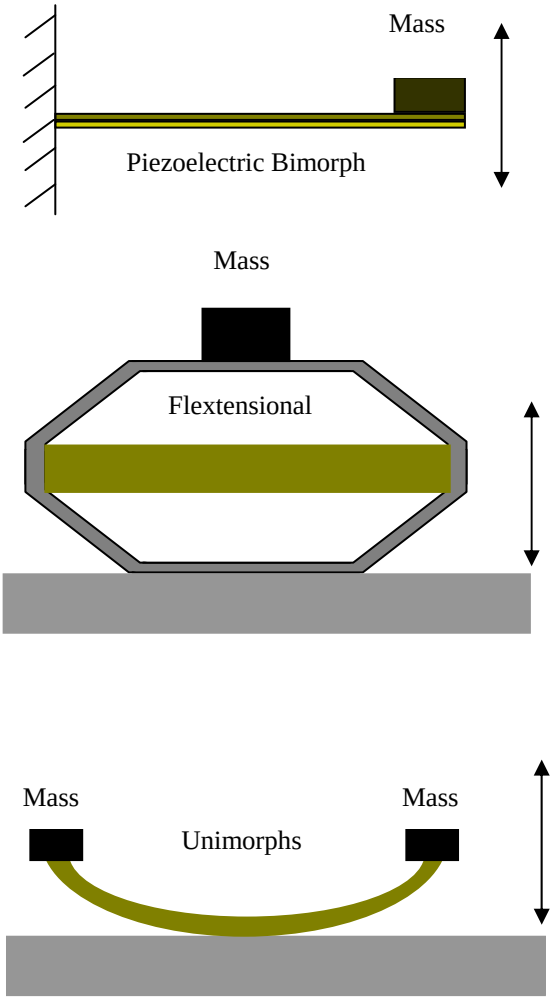

Figure 11. Low resonance frequency piezoelectric transducers.

An example of a full system model that can be used to investigate the power source and structure interaction with the harvester is the acoustic electric feed-through model base on thickness mode excitations shown in Figure 12. In this device we use one piezoelectric to generate a harmonic force which propagates through a structure (wall) and excites the other piezoelectric. Each of the piezoelectrics has a reaction mass on there opposing surfaces. This approach to transmitting energy was first put forth by Hu Et al.[15]. In a later paper an electromechanical model was developed[16] that allowed for the inclusion of losses and adding both mechanical structures and electrical impedances on the electrical port. In the analysis of the structure reported in[15,16] it was found that including the dielectric and the piezoelectric loss decreased the power transfer efficiency by about 20% at resonance and proportionally more between resonances. Increasing the wall Q from a 100 to a 1000 increased the power transfer efficiency by about 10% at resonance. A series of these devices were developed and

tested using thin plates with up to 100 W power transfer. The latest and highest power device we have developed is shown in Figure 13. The transmit piezoelectric and the receive piezoelectric consisted of a set of six 50 mm diameter 5mm thick PZT 8 rings separated by a titanium wall. The PZT was pre-stressed to keep the piezoelectric in compression during operation using high performance steel alloy bolts (SPS Technologies #MP35N).

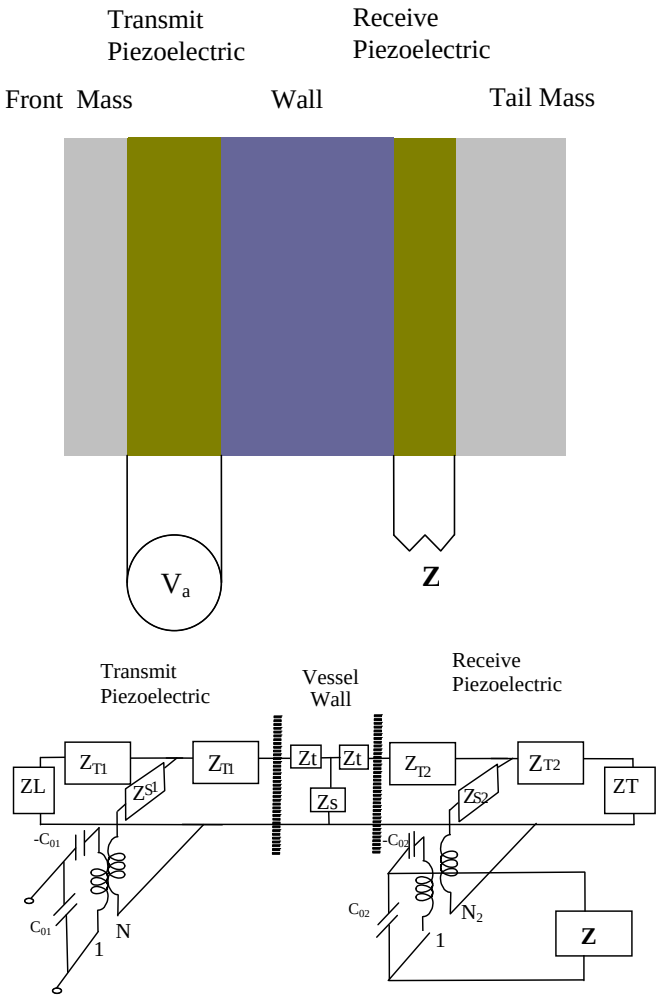

Figure 12. A schematic diagram of the acoustic electric feed-through and the matching equivalent circuit.

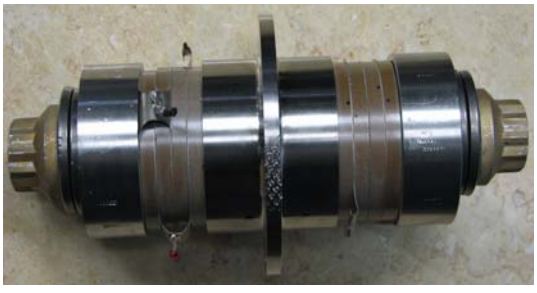

Figure 13. A photograph of a high power acoustic electric feed-through prototype. The final design had six piezoelectric rings.

The device was shown to transmit 1068 W at 16 kHz with 84% efficiency. A series of 10 – 100 W light bulbs were driven using the electrical output of the feed-through. The overall power density was 70 W/cm^2 and 25 W/cm^3. The power density is found to be a maximum for a given load resistance when the mechanical energy density in the piezoelectric is a maximum. In all the systems we have discussed the approach has been to increase the force experienced by the piezoelectric to increase the power density. Whether this is by mechanically clamping, mass clamping or resonance clamping the peak power density occurs when the mechanical energy density is a maximum.

3. DISCUSION

As was noted above, to maximize the extractable power density in a harvester device we require the maximization of the mechanical energy density in the piezoelectric material. In the analysis we used the small signal material constants however to maximize the mechanical energy density we require stresses up to prestress levels (15 to 30 MPa). Ideally we require the material coefficients as evaluated at the stress and field levels in the device. To first order and in the limit that the linear relationships relating the field variables do not exhibit pinching and saturation one could use Rayleigh's law[42] to determine effective complex material constants at these high drive levels. In addition it should be noted that irreversible effects such as de-poling can occur at low frequency stress levels of the order of 30 MPa - 80 MPa depending on whether the PZT is hard or soft[43] (Coercive field high or low). It should also be noted that the interface between the structure and the harvester is also important for higher frequency devices[44].

Typical power requirements[5,45] for a variety of electronic devices are shown in Figure 14. As can be seen in the figure many devices can easily be powered by μW- mW energy harvesters.

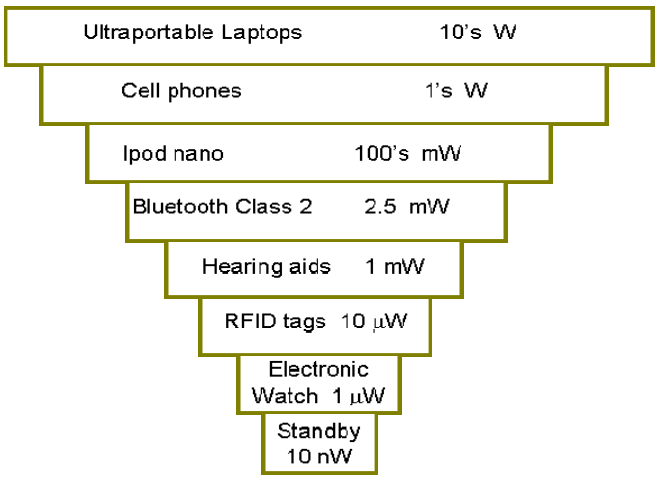

Figure 14. Power requirements for a variety of electronic devices.

The utility of converting energy/power of mechanical vibrations to electrical energy using piezoelectrics depends on the mechanical power, elastic or kinetic, in the structure. Examples of where one can find significant mechanical energy densities in the 10-1000 Hz frequency range include bridge trusses, engine mounts, wheels, roadways, etc. How far up the inverted power pyramid shown in Figure 14 one can climb by harnessing energy from these structures depends on a variety of factors including cost, mass, volume available. Although much of the technical details of this field have been developed more effort is required in developing niche applications for this technology. It is clear however that due to the reduction of power required by modern electronics a host of potential applications can be powered by these transducers especially in enclosed, isolated and rotating structures.

Another potential source that has been proposed is human power[1,3,8,11]. The frequency of mechanical forces produced by the human body is of the order of a few Hz for arm and leg motion, breathing, heartbeats, blood pressure[5]. In addition the power levels required are not insignificant. For example walking requires greater than 100 W [46]of pure mechanical energy while the heart produces 1-2 W of mechanical power[47]. It has been estimated that harvesters based on walking could produce about 7 W of electrical power and current technology can produce about 1 W[2]. It should be noted that muscles are only about 20%[46] efficient so the limit of power extraction for these devices will be when they become a burden for the person. Harvesting power internal to the body has even stricter requirements in that constricting blood flow or heart muscle movement or breathing by even 5% could have dire short and long term consequences for the normal functioning of the body. In each case the limiting power requirement on the system should be that the harvester is unobtrusive.

In the analysis of the models we looked at ways to reduce the source impedance of the piezoelectric to aid in matching to storage circuitry. An alternative approach is to use non-linear matching circuits[5,6,7,8] that can operate over a wide bandwidth. This approach is advantageous since most structures that can be acoustically harvested have acoustic power spectra. Another alternative is to use multimode resonators[48] with overlapping bandwidth. These devices utilize geometric scaling of the resonators to produce overlapping resonances to broaden the bandwidth.

For a given frequency below resonance and a set force or displacement a figure of merit can be determined using equations 1 or 2 with the short circuit elastic constant. The maximum power amplitude can be determined from these equations by noting $P(\omega) = V(\omega)^2/R_L$ and taking the derivative with respect to R_L. The max power condition is found when $R_L=|\mathbf{Z}_0|$. Using the impedance at maximum power we find for the lossless case that

$$P \propto \frac{k_t^2}{\left(1-k_t^2\right)c_{33}^E} \tag{4}$$

for the thickness mode and the harvester power increases as the coupling increases and the stiffness decreases. It should be noted that in a full design of a harvesting system one should include the structure as well to take into effect the difference in stiffness and density. Since most structures and harvester materials have similar acoustic impedances the effect of impedance mismatch is not of general concern however in some instances this may not be a good assumption and one should account for a possible acoustic impedance mismatch.

4. CONCLUSIONS

We have used the piezoelectric equivalent circuit model of Mason to investigate the physical acoustics of energy harvesting systems and how they may be optimized. In the off resonance mode the power density was shown to be controlled by the short circuit elastic constant at impedances below matching impedance and the open circuit elastic constant above. We investigated clamped structures and suggested that the power density could be increased by funneling the stress in the structure through the piezoelectric. In the free structures we looked at adding a reaction mass to increase the force experienced by the piezoelectric and increase the energy density. The use of multilayers to decrease the source impedance and allow for inductive tuning was also reported. Resonance clamping and the impetus for using low frequency resonators was also discussed. Although these techniques and the inductive tuning can be designed to increases the generated power for a small frequency band. They have the disadvantage of narrowing the bandwidth of the conversion. The guiding principal to maximize the power density was found to be to increase the input mechanical energy density by maximizing the stress in the piezoelectric.

ACKNOWLEDGEMENTS

The author would like to thank Dr's Xiaoqi Bao, Mircea Badescu, Yoseph Bar-Cohen, Jack Aldrich and Zensheu Chang for useful discussions. Research reported in this manuscript was conducted at the Jet Propulsion Laboratory (JPL), California Institute of Technology, under a contract with National Aeronautics Space Administration (NASA).

REFERENCES

[1]S.R. Platt, S. Farriator, H. Haider, "On Low-Frequency Electric Power Generation With PZT Ceramics", IEEE/ASME Transactions on Mechatronics, **10**, pp. 240-252, April 2005

[2]J. A. Paradiso, T. Starner, "Energy Scavenging for Mobile and Wireless Electronics", *IEEE Pervasive Computing*, **4**, 1, pp. 18-27. 2005

[3]N. Shenck, , "A Demonstration of Useful Electric Energy Generation from Piezoceramics in a Shoe", MS Thesis, Dept. of Electric Engineering and Computer Science, Massachusetts Institute of Technology, April 1998

[4]S.K. Moore," Printing Technology Makes Miniature Energy Harvesters, Antennas, and Fuel-Cell Parts", IEEE Spectrum Online, February 2008, See [Downloaded Oct/2008] **http://www.spectrum.ieee.org/feb08/5959** and **http://www.spectrum.ieee.org/feb08/5942**
[5]S. Priya, "Advances in energy harvesting using low profile piezoelectric transducers", J Electroceram **19**, pp. 165–182, 2007
[6]D. Guyomar, A. Badel, E. Lefeuvre, C. Richard," Toward Energy Harvesting Using Active Materials and Conversion Improvement by Nonlinear Processing", IEEE Trans. UFFC, **52**, pp. 584-595, April 2005
[7]M. Lallart, L. Garbuio, L. Petit, C. Richard, D. Guyomar, "Double Synchronized Switch Harvesting (DSSH): A New Energy Harvesting Scheme for Efficient Energy Extraction" IEEE Trans. UFFC, **55**, pp. 2119-2130, Oct 2008
[8]N. S. Shenck, J. A. Paradiso, "Energy Scavenging With Shoe-Mounted Piezoelectrics", IEEE MICRO, May-June, pp. 30-42, 2001
[9]IEEE Spectrum, pp. 72, Feb 2008
[10]R. Stevenson, "First Solar: Quest for the $1 Watt", IEEE Spectrum, August 2008
[11]E.K Reilly, E. Carleton, and P. K. Wright" Thin Film Piezoelectric Energy Scavenging Systems for Long Term Medical Monitoring", Proceedings of the International Workshop on Wearable and Implantable Body Sensor Networks (BSN'06), IEEE Computer Society, Boston, MA, April 2006
[12]T. Kaya, H. Koser, "A New Batteryless Active RFID System: Smart RFID", *RFID Eurasia, 2007 1st Annual* , vol., no., pp.1-4, 5-6 Sept. 2007
[13]N.W. Hagood and A. von Flotow, Damping of structural vibrations with piezoelectric materials and passive networks. Journal of Sound and Vibration **146,** 2, pp. 243–268, 1991
[14]C. Richard, D. Guyomar, D. Audigier and G. Ching, Semi-passive damping using continuous switching of a piezoelectric device. Proc. of SPIE Conference on Passive Damping and Isolation **3672**, SPIE, California, USA (1999), pp. 104–111.
[15]Y. Hu, X. Zhang, J. Yang, Q. Jiang, " Transmitting Electric Energy Through a Metal Wall by Acoustic Waves Using Piezoelectric Transducers, IEEE Transactions on Ultrasonics, Ferroelectrics, and Frequency Control, **50**, 7, pp. 773-781, 2003
[16]S. Sherrit, M. Badescu, X. Q. Bao, Y. Bar-Cohen, and Z. Chang, "Efficient electromechanical network model for wireless acoustic-electric feed-throughs," Proceeding of the Smart Sensor Technology and Measurement Systems Conference, SPIE Smart Structures and Materials Symposium, **5758**-44, San Diego, CA, March 7 - 10, 2005.
[17]X. Bao, W. Biederman, S. Sherrit, M. Badescu, Y. Bar-Cohen, C. M. Jones, J. B. Aldrich, Z. Chang, "High-power piezoelectric acoustic electric power feedthru for metal walls" Proceedings of the SPIE 15th International Symposium on Smart Structures and Materials, San Diego, CA, SPIE Vol. **693**0-36, 9-13 March, 2008
[18]X. Bao, B. J. Doty, S. Sherrit, M. Badescu, Y. Bar-Cohen, J. Aldrich, and Z. Chang "Wireless piezoelectric acoustic-electric power feedthru" Proceedings of the SPIE 14th International Symposium on Smart Structures and Materials, San Diego, CA, SPIE Vol. **6529**-134, 18-22 March, 2007.
[19]D.A. Berlincourt, D.R. Curran, H. Jaffe, Physical Acoustics I Part A Chapter 3, " Piezoelectric and Piezomagnetic Materials and their Function in Transducers", pp. 169-270, Academic Press, W.P. Mason,- editor, 1964
[20]S. Sherrit, S.P. Leary, B. Dolgin, Y. Bar-Cohen, "Comparison of the Mason and KLM Equivalent Circuits for Piezoelectric Resonators in the Thickness Mode", Proceedings of the IEEE Ultrasonics Symposium, pp. 921-926 , Lake Tahoe, Oct 1999,
[21]M. Redwood, "Transient Performance of a Piezoelectric Transducer", Journal of the Acoustical Society of America, **33**, pp.527-536, 1961
[22]H.J. McSkimmin , "Chapter 4- Ultrasonic Methods for Measuring the Mechanical Properties of Liquids and Solids, pp. 271-334, Physical Acoustics-*Principles and Methods*, Volume 1-Part A, ed. W.P. Mason Academic Press, New York, 1964
[23]D.J. Powell, G. L. Wojcik C. S. Desilets, T.R. Gururaja, K. Guggenberger, S. Sherrit, B.K. Mukherjee, "Incremental "Model-Build-Test" Validation Exercise For a 1-D Biomedical Ultrasonic Imaging Array", Proceedings of IEEE Ultrasonics Symposium, Vol 2, pp. 1669- 1674, Toronto, Oct 1997
[24]S. Sherrit, H.D. Wiederick, B.K. Mukherjee, M. Sayer, "A Complete Characterization of the Piezoelectric, Dielectric, and Elastic Properties of Motorola PZT 3203 HD including Losses and Dispersion" , Proceedings of the International Society for Optical Engineering Symposium on Medical Imaging, Vol. **3037**, pp. 158-169 Feb, 1997
[25]D.J. Powell, G. L. Wojcik C. S. Desilets, T.R. Gururaja, K. Guggenberger, S. Sherrit, B.K. Mukherjee, "Incremental "Model-Build-Test" Validation Exercise For a 1-D Biomedical Ultrasonic Imaging Array", Proceedings of IEEE Ultrasonics Symposium, Vol 2, pp. 1669- 1674, Toronto, Oct 1997
[26]S. Sherrit, H.D. Wiederick, B.K. Mukherjee, M. Sayer, "A Complete Characterization of the Piezoelectric, Dielectric, and Elastic Properties of Motorola PZT 3203 HD including Losses and Dispersion" , Proceedings of the International Society for Optical Engineering Symposium on Medical Imaging, Vol. **3037**, pp. 158-169 Feb, 1997
[27]Acoustic properties Material datasheet, Onda Corportation, http://www.ondacorp.com/tables/Solids.pdf, Downloaded Oct 10, 2008
[28]G.E. Martin, "Vibrations of Coaxially Segmented Longitudinally Polarized Ferroelectric Tubes", JASA **36**, pp. 1496-1506, August 1964.

[29]G.E. Martin, “On the Theory of Segmented Electromechanical Systems” JASA, 36, pp 1366-1370.
[30]S. Sherrit, S.P. Leary, B.P. Dolgin, Y. Bar-Cohen, R. Tasker, "The Impedance Resonance for Piezoelectric Stacks", Proceedings of the IEEE Ultrasonics Symposium in San Juan, Puerto Rico, Oct 22-25, 2000
[31]Q.M. Wang,Q. Zhang, B. Xu, R. Liu, L. E.Cross, “Nonlinear piezoelectric behavior of ceramic bending mode actuators under strong electric fields” J. Appl. Phys., 86, 6, pp.3352-3360, 1999
[32]H.U.Kim, V. Bedekar, R. A. Islam, W.H. Lee, D. Leo, and S. Priya,” Laser-Machined Piezoelectric Cantilevers for Mechanical Energy Harvesting”, IEEE Transactions on Ultrasonics, Ferroelectrics, and Frequency Control, **55**, 9, pp.1900-1905, 2008
[33]J. G. Smits and W.S. Choi, ” The Constituent Equations of Piezoelectric Heterogeneous Bimorphs”, IEEE Transactions on Ultrasonics, Ferroelectrics, and Frequency Control, **38**, 3, pp.256-270, 1991
[34]R. Le Letty, F. Claeyssen,F. Barillot, and N. Lhermet, “Amplified Piezoelectric Actuators for aerospace applications”, AMAS Workshop on Smart Materials and Structures SMART’03, pp.51–62, Jadwisin, September, 2003
[35]H. W. Kim, A. Batra, S. Priya, K. Uchino, D. Markley, R. E. Newnham and H. F. Hofmann,” Energy Harvesting Using a Piezoelectric ‘‘Cymbal’’ Transducer in Dynamic Environment”, Japanese Journal of Applied Physics, 43, 9A, pp. 6178–6183, 2004
[36]G. H. Haertling,” Rainbow actuators and sensors: a new smart technology”, Proc. SPIE, Vol. **3040**, 81 (1997)
[37]B. W. Barron, G. Li, G.H. Haertling, “Temperature dependent characteristics of Cerambow actuators”, Proceedings of the Tenth IEEE International Symposium on Applications of Ferroelectrics, East Brunswick, NJ, USA, 1996. ISAF '96.,
[38]FACE International Corporation, Norfolk, VA 23508
[39]Y. S. Cho , Y. E. Pak , C. S. Han, S. K. Ha,” Five-port equivalent electric circuit of piezoelectric bimorph beam”, Sensors and Actuators, **84**, pp. 140–148, 2000
[40]J.-C. Debus, B. Hamonic, B. Damiri, “Analysis of a Flextensional Transducer Using Piece-Part Equivalent Circuit Models: Determination of the Shell Contribution”, Proceedings of OCEANS 94. 'Oceans Engineering for Today's Technology and Tomorrow's Preservation.', pp. 289-294, vol.2, Brest France, 1994
[41]A.R.D. Curtis,” Active Control of Fan Noise by Vane Actuators”, NASA CR, 209-156, 1999, Downloaded Oct 2008 http://ntrs.nasa.gov/archive/nasa/casi.ntrs.nasa.gov/19990047908_1999064353.pdf,
[42]D. Damjanovic, “Chapter 4 - Hysteresis in Piezoelectric and Ferroelectric Materials”, The Science of Hysteresis, Volume 3; I. Mayergoyz and G.Bertotti (Eds.); Elsevier (2005)
[43]G. Yang, S. F. Liu, W. Ren, and B. K. Mukherjee, ”Uniaxial stress dependence of the piezoelectric properties of lead zirconate titanate ceramics”, Proc. SPIE **3992**, 103 (2000)
[44]S. Sherrit, B. Doty, M. Badescu, X.Bao, Y.Bar-Cohen, J. Aldrich, Z. Chang,”Studies of Acoustic-Electric Feed-throughs for Power Transmission Through Structures”, Smart Structures and Materials 2006: Industrial and Commercial Applications of Smart Structures Technologies, edited by Edward V. White, Proc. of SPIE Vol. 6171, 617102, (2006) ·
[45]G. Sebald, E. Lefeuvre, D. Guyomar, “Pyroelectric Energy Conversion: Optimization Principles” IEEE Transactions on Ultrasonics, Ferroelectrics, and Frequency Control, **55**, 3, pp. 538-551, 2008
[46]A. Bellemans,” Power Demands in Walking and Pace Optimizaton, pp. 117- 119, The Physics of Sports , Ed. Angelo Armenti Jr. Springer, 1991
[47] K.R. Koehler, The human cardiovascular system, http://www.rwc.uc.edu/koehler/biophys/3a.html, Downloaded Oct, 2008
[48]H. Xue, Y. Hu, and Q. M. Wang,” Broadband Piezoelectric Energy Harvesting Devices Using Multiple Bimorphs with Different Operating Frequencies”, IEEE Transactions on Ultrasonics, Ferroelectrics, and Frequency Control, 55, 9, pp.2104-2108, 200835